Chapter 13
Hume–Rothery Stabilization Mechanism of Be-Based Complex Alloys

H. Sato, M. Inukai, E.S. Zijlstra, and U. Mizutani

Abstract We performed first-principles FLAPW (Full potential Linearized Augmented Plane Wave) band calculations for $Be_{13}Mg$ and $Be_{13}Sb$. Furthermore, we calculated the Hume–Rothery plot and $\mathbf{e/a}$ with the tetrahedron method from the case.output1 file generated from WIEN2k. These complex alloys belong to fcc structures with almost the same atom density as hcp Be. From the FLAPW-Fourier spectrum, we could point out that, in both alloys, the pseudogap is formed by Fs–Bz interactions with the spheres just coinciding to reciprocal lattice vectors, $|\mathbf{G}| = 32, 35, 36$ and 40.

13.1 Introduction

Both the Fermi surface–Brillouin zone (Fs–Bz) interactions and orbital hybridizations have been considered to be responsible for the formation of a pseudogap across the Fermi level in structurally complex metallic alloys (CMAs) [1]. Research along this line had been initiated in the framework of the nearly free electron (NFE) model and later the linear muffin-tin orbital-atomic sphere approximation [2]. The NFE model has a serious drawback since it cannot properly handle transition metals (TM) bearing localized d-band near the Fermi level. To overcome this difficulty, Mizutani and co-workers employed first-principles FLAPW band calculations and established a powerful technique named the FLAPW-Fourier method to extract Fs–Bz interac-

H. Sato (✉)
Aichi University of Education, Kariya-shi, Aichi 448-8542, Japan
e-mail: hsato@auecc.aichi-edu.ac.jp

M. Inukai
Toyota Technological Institute, Hisakata, Tempaku-ku, Nagoya 468-8511, Japan

E.S. Zijlstra
Theoretical Physics, University of Kassel, 34132 Kassel, Germany

U. Mizutani
Nagoya Industrial Science Research Institute, 1-13 Yotsuya-dori, Chikusa-ku, Nagoya 464-0819, Japan

S. Schmid et al. (eds.), *Aperiodic Crystals*, DOI 10.1007/978-94-007-6431-6_13,

tions even in strongly hybridizing CMAs [3–5]. The square of the effective Fermi diameter $(2k_F)^2$ and the number of itinerant electrons per atom $\mathbf{e}/\mathbf{a}$ can be determined by extracting major plane waves of itinerant electrons outside the muffin-tin spheres and subsequently averaging the square of the wave vectors at the Fermi level. The method above has been specifically named the Hume–Rothery plot (hereafter abbreviated as the HR plot), since it can determine the $\mathbf{e}/\mathbf{a}$ value serving as a key parameter in the Hume–Rothery electron concentration rule. Using the HR plot method, they could determine $\mathbf{e}/\mathbf{a}$ values even for TM metals and their alloys [6], which had been a longstanding subject in the electron theory of metals since the 1930s [7, 8].

In the present work, attention is directed to the $Be_{13}X$ (X = Mg, Ca, Zr, Sb and La) compounds containing 112 atoms per unit cell (cF112) with space group $Fm\bar{3}c$. The structure information of $Be_{13}X$ compounds is available in the literature [9]. They are characterized by a deep pseudogap across the Fermi level. Our objective is to discuss the origin of the pseudogap from the viewpoint of Fs–Bz interactions by applying the FLAPW-Fourier analysis to $Be_{13}Mg$ and $Be_{13}Sb$, both of which are composed of only sp-bands.

We have recently established the tetrahedron method to enhance the accuracy in the HR plot method. Its principles will be described in Sect. 13.2. We have performed the HR plot analysis for not only fcc-$Be_{13}Mg$ and $Be_{13}Sb$ but also for hcp-Be, hcp-Mg, trigonal-Sb as references.

13.2 Electronic Structure Calculations

FLAPW band calculations have been executed with INTEL version Linux personal computers by using the WIEN2k program package [10]. It provides us the list of the jth eigenvalue $E^j_{\mathbf{k}}$ and the corresponding Fourier coefficient $C^j_{\mathbf{k}+\mathbf{G}}$ of an allowed reciprocal lattice vector $\mathbf{G}$ for the wave vector $\mathbf{k}$ in the irreducible wedge of the first Brillouin zone.

The tetrahedron method is newly developed for extracting the set of LAPW states having the largest Fourier coefficient $|C^j_{\mathbf{k}+\mathbf{G}}|^2_{\max}$. The values of $E^j_{\mathbf{k}}$ and $C^j_{\mathbf{k}+\mathbf{G}}$ for any $\mathbf{k}$ point in the Brillouin zone of the parallelepiped are replaced by those for the equivalent $\mathbf{k}$ point in the irreducible wedge of the zone, by means of symmetry operations in a given crystal structure. The wedge is further divided into the assembly of tetrahedra. The LAPW state $\{2|\mathbf{k}+\mathbf{G}|\}^2_E$ having $|C^j_{\mathbf{k}+\mathbf{G}}|^2_{\max}$ is calculated at the centre of gravity of each cross-sectional area $S_\ell(E)$ formed by cutting the ℓth tetrahedron through a given energy surface E, using a linear interpolation approximation [11], and is averaged over all the tetrahedra in the Brillouin zone:

$$\left\langle \left\{2|\mathbf{k}+\mathbf{G}|\right\}^2 \right\rangle_E = \frac{\sum_{\ell \text{ in BZ}} \frac{\{2|\mathbf{k}^\ell_{\text{cg}}+\mathbf{G}|\}^2 S_\ell(E)}{|\nabla E|_\ell}}{\sum_{\ell \text{ in BZ}} \frac{S_\ell(E)}{|\nabla E|_\ell}} \tag{13.1}$$

where $\mathbf{k}_{\mathrm{cg}}^{\ell}$ specifies the wave vector at the centre of gravity (cg) of $S_\ell(E)$. The number of itinerant electrons per atom $\mathbf{e}/\mathbf{a}$ is calculated from

$$\left(\frac{e}{a}\right)_{\mathrm{local}} = \frac{\pi}{3N_{\mathrm{atom}}}\left[\frac{V_{\mathrm{uc}}^{3/2}}{4\pi^2}\langle\{2|\mathbf{k}+\mathbf{G}|\}^2\rangle_{E_F}\right]^{3/2}, \tag{13.2}$$

where N_{atom} and V_{uc} are the number of atoms per unit cell and the volume of unit cell, respectively.

13.3 Results and Discussions

The HR plot, i.e. the energy dependence of $\frac{V_{\mathrm{uc}}^{3/2}}{4\pi^2}\langle\{2|\mathbf{k}+\mathbf{G}|\}^2\rangle_E$ along with the total and partial DOSs for hcp-Be and hcp-Mg are shown in Figs. 13.1 and 13.2, respectively. A DOS pseudogap of about 5 eV in width is observed across the Fermi level in Be while a free electron-like DOS with small van-Hove singularities is present in Mg. As can be seen in Fig. 13.1, the pseudogap in Be can be ascribed to orbital hybridizations mainly due to the p states in Be. The direct reading of the ordinate at the Fermi level in Be and Mg yield $(2k_F)^2$ of 2.64 and 2.46 in units of $(2\pi/a)^2 \times \sqrt[3]{3a^2/4c^2}$, respectively. The effective $(\mathbf{e}/\mathbf{a})_{\mathrm{local}}$ value is now immediately calculated from Eq. (13.2) to be 2.24 and 2.02, respectively. The HR data points in Mg fall on a straight line from the bottom of the valence band up to +10 eV. The resulting electronic parameters $(2k_F)^2$ and $(\mathbf{e}/\mathbf{a})_{\mathrm{local}}$ are in perfect agreement with the free electron value.

In the case of Be, we obtained an almost +10 % deviation from the nominal valence of two. The enhancement in $\mathbf{e}/\mathbf{a}$ is explained in terms of the existence of strong orbital hybridization effects in Be. Note that almost 70 % of valence electrons reside inside the MT-sphere of 2 Å in radius while the remaining 30 % as plane waves in intermediate regions. The p-states in the neighbouring Be atoms are hybridized via plane waves in intermediate regions strongly enough to split them into bonding and anti-bonding states across the Fermi level. This effect is reflected in the HR plot as an upward deviation from otherwise the free electron behaviour, as is drawn with red in colour in Fig. 13.1. Similarly, the HR plot for trigonal Sb known as a semimetal provided the value of $(\mathbf{e}/\mathbf{a})_{\mathrm{local}}$ which is 0.33 larger than its nominal valence of five due to strong hybridization effects between the p-states in the same way as in Be.

Now we are ready to discuss Fs–Bz interactions in $Be_{13}Mg$ and $Be_{13}Sb$. As shown in Fig. 13.3, we found the DOS pseudogap in Be to remain essentially unchanged except for the growth of new states immediately above the Fermi level in fcc-$Be_{13}Mg$. A horizontal line with small open circles at both ends in Fig. 13.3 refers to bonding and anti-bonding states caused by the zone splitting associated with $\{2|\mathbf{k}+\mathbf{G}|\}^2 = G^2$ (see Fig. 13.3). It is clear that electronic states over the energy range, where both the pseudogap and the new states are involved, are dominated by those specified by $G^2 = 35$, 36 and 40 in units of $(2\pi/a)^2$.

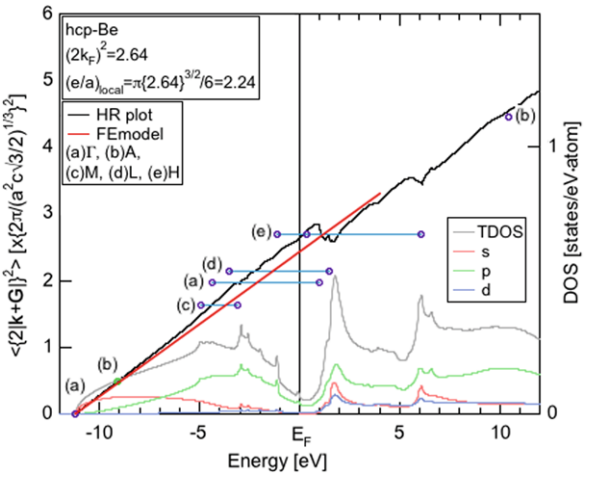

Fig. 13.1 Hume–Rothery plot, and total and partial densities of states for hcp Be. *Small open circles* denote the electronic state $|\mathbf{G}|^2$ versus the energy eigen value at given symmetry points, at which the square of the Fourier coefficient $|C^j_{\mathbf{G}}|^2$ is the largest in the wave function outside the MT sphere

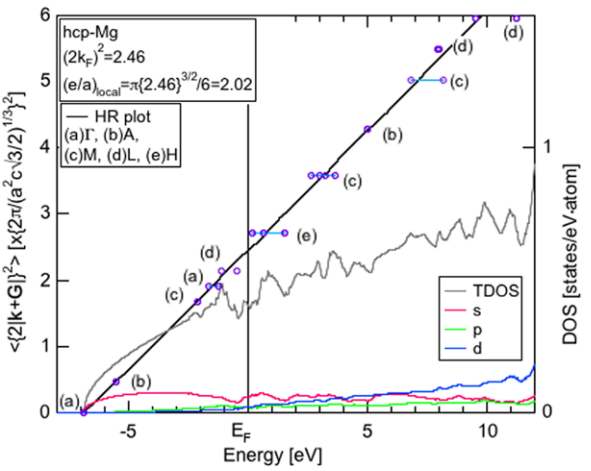

Fig. 13.2 Hume–Rothery plot, and total and partial densities of states for hcp Mg. *Small open circles* denote the electronic state $|\mathbf{G}|^2$ versus the energy eigen value at given symmetry points, at which the square of the Fourier coefficient $|C^j_{\mathbf{G}}|^2$ is the largest in the wave function outside the MT sphere

The HR plot data deviate from otherwise the free electron-like straight line (see the red line in Fig. 13.3) from -3 up to -1 eV but resume the free electron behaviour across the Fermi level. The square of the Fermi diameter $(2k_F)^2 = \langle\{2|\mathbf{k}+\mathbf{G}|\}\rangle^2_{E_F}$ can be read off from the ordinate and turned out to be 35.92. This means that the Fermi surface lies in contact with the zones formed by $|\mathbf{G}|^2 = 35$ and 36, indicating the fulfillment of the matching condition $(2k_F)^2 = |\mathbf{G}|^2$ in the compound $Be_{13}Mg$. The $(\mathbf{e}/\mathbf{a})_{\text{local}}$ value is calculated to be 2.01, which is very close to its nominal value of two: $(\mathbf{e}/\mathbf{a})_{\text{Be}} = (\mathbf{e}/\mathbf{a})_{\text{Mg}} = 2.0$. We consider this to be brought about by the restoration of the free electron behaviour at the Fermi level, thanks to the growth of new states arising from orbital hybridizations between Mg-p and Be-p states.

The HR plot data along with the total DOS for $Be_{13}Sb$ are shown in Fig. 13.4. The total DOS is again found to be similar to that in Be except for the growth of new states across the Fermi level. The growth of the new states must be attributed

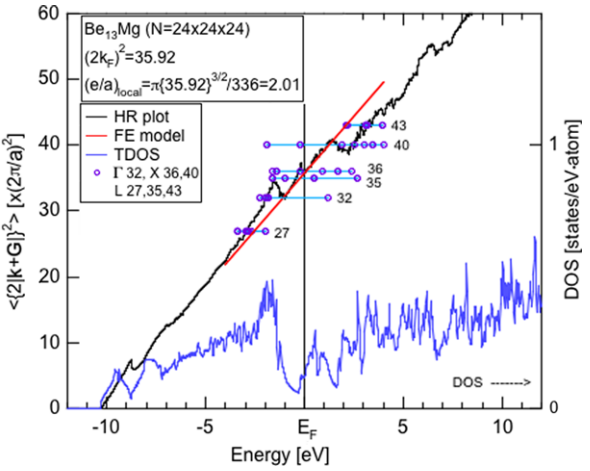

Fig. 13.3 Hume–Rothery plot, and total density of states for $Be_{13}Mg$. *Small open circles* denote the electronic state $|\mathbf{G}|^2$ versus the energy eigen value at given symmetry points, at which the square of the Fourier coefficient $|C_{\mathbf{G}}^{j}|^2$ is the largest in the wave function outside the MT sphere

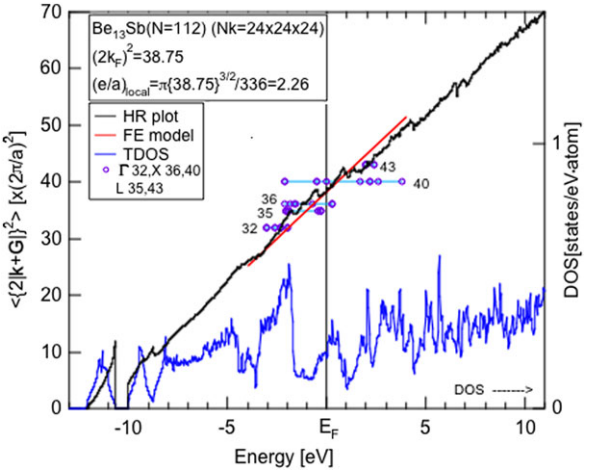

Fig. 13.4 Hume–Rothery plot, and total density of states for $Be_{13}Sb$. *Small open circles* denote the electronic state $|\mathbf{G}|^2$ versus the energy eigen value at given symmetry points, at which the square of the Fourier coefficient $|C_{\mathbf{G}}^{j}|^2$ is the largest in the wave function outside the MT sphere

to orbital hybridization effect between Be-p and Sb-p states. One can see that the free electron-like behaviour, as guided by the red line in Fig. 13.4, is resumed across the Fermi level owing to the growth of the new states. The value of $(2k_F)^2$ is immediately deduced to be 38.75 from the HR plot. The resulting $(\mathbf{e}/\mathbf{a})_{\text{local}} = 2.26$ is very close to its nominal valence of 2.21 (=31/14), lending strong support to the restoration of the free electron behaviour at the Fermi level.

Guided by the same symbols as those in Fig. 13.3, we are convinced to say that electronic states over energies from -2 to $+2$ eV are heavily perturbed by zone effects associated with $G^2 = 35$, 36 and 40, thereby resulting in not only a wide pseudogap but also the new states near the Fermi level inside the pseudogap. In other words, Fs–Bz interactions involving multi-zones of $G^2 = 35$, 36 and 40 are to produce a wide pseudogap as a result of interference of electrons with relevant zone planes in the fcc Brillouin zone.

The Fs–Bz interactions in hcp-Be and Mg essentially involve a single zone of $G^2 = 1.98$ and 1.90, respectively. Instead, the participation of multi-zones is essential upon forming a pseudogap in CMAs including $Be_{13}Mg$ and $Be_{13}Sb$.

In summary, we revealed that the effective Fermi spheres with $(2k_F)^2 = 35.92$ and 38.75 for $Be_{13}Mg$ and $Be_{13}Sb$, respectively, are embedded in the net of almost spherical Brillouin zones consisting of 12-fold {440} with $G^2 = 32$, 48-fold {531} with $G^2 = 35$, 8-fold {600} and 24-fold {442} zones with $G^2 = 36$ and 24-fold {620} zones with $G^2 = 40$. The Fs–Bz interactions involving the multi-zones above must be responsible for forming a pseudogap and new states as well across the Fermi level and thereby lowering the electronic energy of the system. The involvement of the common Fs–Bz interactions in them leads us to conclude that they obey the Hume–Rothery stabilization mechanism, though the multi-zone effect causes the resulting $(\mathbf{e}/\mathbf{a})_{\text{local}}$ values to be scattered over 2.01 to 2.26.

References

1. Mizutani U (2010) Hume–Rothery rules for structurally complex alloy phases. CRC Press/Taylor & Francis Group, Boca Raton
2. Sato H, Takeuchi T, Mizutani U (2004) Phys Rev B 70:094207
3. Asahi R, Sato H, Takeuchi T, Mizutani U (2005) Phys Rev B 71:165103
4. Asahi R, Sato H, Takeuchi T, Mizutani U (2005) Phys Rev B 72:125102
5. Mizutani U, Asahi R, Sato H, Takeuchi T (2006) Phys Rev B 74:235119
6. Mizutani U, Inukai M, Sato H, Zijlstra ES (2012) Philos Mag 92:1691
7. Pauling L (1938) Phys Rev 54:899
8. Raynor GV (1949) Prog Met Phys 1:1
9. Beker TW (1962) Acta Crystallogr 15:175
10. Blaha P, Schwarz K, Madsen G, Kvasnicka D, Luitz J. http://www.wien2k.at/
11. Lehman G, Taut M (1972) Phys Status Solidi (b) 54:469